DALTON
FULL PAPER

Stereochemistry and electrochemical properties of molybdenum ions incorporated into S-bridged polynuclear structures

Yoshitaro Miyashita,*[a] Yasunori Yamada,[a] Kiyoshi Fujisawa,[a] Takumi Konno,[b] Kan Kanamori[c] and Ken-ichi Okamoto*[a]

[a] *Department of Chemistry, University of Tsukuba, Tsukuba, Ibaraki 305-8571, Japan. E-mail: okamoto@staff.chem.tsukuba.ac.jp*
[b] *Department of Chemistry, Faculty of Engineering, Gunma University, Kiryu, Gunma 376-8516, Japan*
[c] *Department of Chemistry, Faculty of Science, Toyama University, Toyama, Toyama 930-8555, Japan*

Received 17th August 1999, Accepted 9th February 2000

The reactions of *fac*(*S*)-[M(aet)$_3$] (M = Ir^{III} or Rh^{III}; aet = 2-aminoethanethiolate) with [NH$_4$]$_2$[MoCl$_5$(H$_2$O)] in both anaerobic and aerobic atmospheres gave linear-type S-bridged trinuclear complexes, [Mo^{IV}{Ir(aet)$_3$}$_2$]$^{4+}$ **1** and [Mo^{III}{Rh(aet)$_3$}$_2$]$^{3+}$ **2**. Complex **2** was spontaneously oxidized by exposure to air and converted into a novel S-bridged pentanuclear complex, [Mo$^{V}_2$O$_2$(μ-O){Rh(aet)$_3$}$_3$]$^{4+}$ **3**, and the structural change from **2** to **3** was monitored by UV-vis spectroscopy. The crystal structures of **1**Br$_4$·4H$_2$O, **2**Br$_3$·H$_2$O, and **3**Br$_4$·6H$_2$O were determined by X-ray diffraction. In the complex cations **1** and **2**, Mo^{4+} and Mo^{3+} ions are co-ordinated by the six thiolato sulfur atoms from two *fac*(*S*)-[M(aet)$_3$] units and relatively short metal–metal distances (2.7469(7) and 2.860(3) Å) are observed, respectively. In **3** the Mo–O–Mo angle (157.0(4)°) in the Mo$_2$O$_2$(μ-O)$^{4+}$ core is unique and the core is co-ordinated by the eight thiolato sulfur atoms of three *fac*(*S*)-[Rh(aet)$_3$] units. The cyclic voltammograms for **1** and **2** indicate that the oxidation states of the molybdenum ions, which are incorporated into the S-bridged polynuclear structures, and stability of the complexes, depend upon the metal ions in the terminal building blocks, *fac*(*S*)-[M(aet)$_3$]. The absorption spectrum of each complex exhibited characteristic intense bands in the visible region, which relate to the molybdenum ions.

Introduction

Co-ordinated thiolato sulfur atoms in mononuclear complexes, *fac*(*S*)-[M(aet)$_3$] (M = Ir^{III} or Rh^{III}; aet = 2-aminoethanethiolate), which can be regarded as building blocks for construction of polynuclear complexes, have been recognized to bind with other metal ions to form a variety of S-bridged polynuclear structures.[1–7] The polynuclear structures are highly dependent upon the co-ordination geometry of the reacting metal ions, and the thiolate chemistry of the late transition metal complexes has widely been investigated.[1–6] Recently, we have reported the linear-type trinuclear complexes, [Cr{M(aet)$_3$}$_2$]$^{3+}$ (M = Ir^{III} or Rh^{III}),[7] as the first attempt to incorporate the early transition metal ions into S-bridged polynuclear structures by using the building blocks *fac*(*S*)-[M(aet)$_3$]. These polynuclear chromium(III) complexes have significantly different reactivity and electrochemical properties from the previously reported polynuclear complexes based on late transition metal ions.[1–7] Further, it is known that molybdenum has very different redox and stereochemical properties from chromium in spite of being a congener.[8] In order to elucidate the thiolate chemistry of the early transition metal ions, therefore, we have introduced molybdenum(III) ion into the S-bridged polynuclear systems. This low oxidation state of molybdenum is rare, and it is interesting to see whether it retains the starting trivalent state when incorporated into these S-bridged polynuclear structures. In this paper we report several S-bridged heteropolynuclear complexes, which were obtained by the reactions of *fac*(*S*)-[M(aet)$_3$] (M = Ir^{III} or Rh^{III}) with [NH$_4$]$_2$[MoCl$_5$(H$_2$O)]. The complexes incorporate molybdenum-(III), -(IV), or -(V) ions depending upon the nature of the building blocks *fac*(*S*)-[M(aet)$_3$]. Their stereochemistry and electrochemical properties are discussed.

Experimental

Materials

2-Aminoethanethiol, IrCl$_3$, and RhCl$_3$·*n*H$_2$O were purchased from Tokyo Kasei Kogyo Co., Ltd., Rare Metallic Co., Ltd., and N. E. Chemcat Co., Ltd., respectively. The other reagents were obtained from Wako Pure Chemical Ind. Ltd. All chemicals were of reagent grade and used without further purification.

Preparation of complexes

[NH$_4$]$_2$[MoCl$_5$(H$_2$O)]. This complex was prepared by a modification of the method of Shibahara and Yamazaki.[9] In that paper the preparation of [NH$_4$]$_3$[MoCl$_6$] was described, but [NH$_4$]$_2$[MoCl$_5$(H$_2$O)] was produced without HCl gas.

***fac*(*S*)-[Ir(aet)$_3$]**[6,7] **and *fac*(*S*)-[Rh(aet)$_3$].**[1b,7,10] These complexes were prepared by the methods described in previous papers.

[Mo{Ir(aet)$_3$}$_2$]$^{4+}$ 1. The salt [NH$_4$]$_2$[MoCl$_5$(H$_2$O)] (0.118 g, 0.361 mmol) was dissolved in 3 cm^3 of 1 mol dm^{-3} HBr solution and 1 cm^3 of a saturated NaBr aqueous solution added. To the red solution was added *fac*(*S*)-[Ir(aet)$_3$] (0.300 g, 0.713 mmol) slowly with stirring. The orange mixture was stirred under nitrogen at room temperature for 15 min, whereupon it became a dark brown suspension. The resulting dark brown crystalline powder (**1**Br$_4$·4H$_2$O) was collected by filtration. Yield: 0.411 g (87%). A similar crystalline powder was also obtained by a reaction in air. Found: C, 10.92; H, 3.40; Ir, 28.58; Mo, 6.86; N, 6.21%. [Mo{Ir(aet)$_3$}$_2$]Br$_4$·4H$_2$O =

DOI: 10.1039/a906665i

$C_{12}H_{36}Br_4Ir_2MoN_6S_6\cdot 4H_2O$ requires C, 10.85; H, 3.34; Ir, 28.93; Mo, 7.22; N, 6.32%.

$[Mo\{Rh(aet)_3\}_2]^{3+}$ 2. The complex *fac*(*S*)-[Rh(aet)$_3$] (0.300 g, 0.905 mmol) was dissolved in 5 cm^3 of 1 mol dm^{-3} HBr solution. To the yellow solution was added $[NH_4]_2[MoCl_5(H_2O)]$ (0.150 g, 0.458 mmol) in 2 cm^3 of 1 mol dm^{-3} HBr solution. The orange mixture was stirred under nitrogen at room temperature for 15 min, whereupon it became a green-brown suspension. To this suspension was added 1 cm^3 of a saturated NaBr aqueous solution, followed by stirring for 15 min. After standing in a refrigerator for 3 h, the resulting black micro crystals (**2**$Br_3\cdot H_2O$) were collected by filtration. Yield: 0.422 g (92%). Similar micro crystals were also obtained by a reaction in air. Found: C, 14.05; H, 3.72; Mo, 9.05; N, 8.22; Rh, 19.92%. $[Mo\{Rh(aet)_3\}_2]Br_3\cdot H_2O = C_{12}H_{36}Br_3MoN_6Rh_2S_6\cdot H_2O$ requires C, 14.18; H, 3.77; Mo, 9.44; N, 8.27; Rh, 20.25%.

$[Mo_2O_2(\mu\text{-}O)\{Rh(aet)_3\}_3]^{4+}$ 3. *Method A.* The salt **2**$Br_3\cdot H_2O$ (0.420 g, 0.413 mmol) was dissolved in 30 cm^3 of water. To the greenish brown solution was added a few drops of a saturated NaBr aqueous solution. After standing in a refrigerator for 3 d an insoluble precipitate was removed by filtration. To the resulting wine-red filtrate was added 1 cm^3 of a saturated NaBr aqueous solution. Black crystals (**3**$Br_4\cdot 6H_2O$) appeared upon standing in a refrigerator for 3 d. Yield: 0.247 g (72%).

Method B. The complex *fac*(*S*)-[Rh(aet)$_3$] (0.300 g, 0.905 mmol) was dissolved in 5 cm^3 of 1 mol dm^{-3} HBr solution. To the yellow solution was added $[NH_4]_2[MoCl_5(H_2O)]$ (0.300 g, 0.917 mmol) in 5 cm^3 of 1 mol dm^{-3} HBr solution. The orange mixture was stirred in air at room temperature for 1 d, whereupon it became a wine-red suspension. After adding 1 cm^3 of a saturated NaBr aqueous solution and stirring for 1 d, the resulting wine-red powder (0.503 g) was collected by filtration. To the crude powder was added 50 cm^3 of water and insoluble materials were removed by filtration. To the wine-red filtrate were added 3 cm^3 of a saturated NaBr aqueous solution. The resulting black micro crystals (**3**$Br_4\cdot 6H_2O$) were collected by filtration. Yield: 0.133 g (27%). Found: C, 12.87; H, 4.04; Mo, 10.39; N, 7.47; Rh, 18.25%. $[Mo_2O_2(\mu\text{-}O)\{Rh(aet)_3\}_3]Br_4\cdot 6H_2O = C_{18}H_{54}Br_4Mo_2N_9O_3Rh_3S_9\cdot 6H_2O$ requires C, 13.01; H, 4.00; N, 7.59; Mo, 11.55; Rh, 18.58%.

Measurements

Electronic absorption spectra were recorded with a JASCO V-560 spectrophotometer in aqueous solution at room temperature. The elemental analyses (C, H, and N) were performed by the Analysis Center of the University of Tsukuba. The concentrations of Ir, Rh and Mo in the complexes were determined with a NIPPON Jarrell-Ash ICPA-575 ICP spectrophotometer. The infrared spectra were recorded as KBr disks with a JASCO FT/IR-550 spectrometer, Raman spectra on a JASCO RFT-200 FT-Raman spectrophotometer with excitation by a YAG laser line (1064 nm) and samples were in the form of KBr disks. The molar conductances of the complexes were measured with a HORIBA conductivity meter DS-14 in aqueous solution at room temperature. The magnetic measurements were performed by using a Sherwood Scientific susceptibility apparatus at 23 °C. Diamagnetic corrections employed tabulated constants.[11] Electrochemical measurements were made by a CV-1B apparatus (Bioanalytical Systems, Inc.) using a glassy-carbon working electrode (GCE). An aqueous Ag–AgCl–NaCl (3 mol dm^{-3}) electrode (Bioanalytical Systems, Inc., RE-1) and platinum wire were used as reference and auxiliary electrode, respectively. Electrochemical experiments were conducted in a 0.1 mol dm^{-3} aqueous solution of Na_2SO_4 as a supporting electrolyte and complex concentrations of 1.0 mmol dm^{-3}. Molecular mechanics calculations (MM2 program) were performed on a Power Macintosh computer with the CAChe program.[12]

A solution containing 0.0075 g of $[Mo\{Rh(aet)_3\}_2]^{3+}$ **2** in 0.5 cm^3 of water was exposed to air with stirring at room temperature for a definite time. The solution was filtered and the filtrate diluted to 25 cm^3 by 1 mol dm^{-3} HCl solution, and then the absorption spectrum was measured on a JASCO V-560 spectrophotometer.

Crystallography

Single crystals of complexes **1**$Br_4\cdot 4H_2O$, **2**$Br_3\cdot H_2O$, and **3**$Br_4\cdot 6H_2O$ suitable for X-ray analysis were obtained by recrystallization from water by adding a few drops of a saturated NaBr aqueous solution. Unit cell and intensity data were collected on a Rigaku AFC-7S four-circle diffractometer (Mo-Kα radiation, ω–2θ scan mode, $2\theta_{max} = 55°$, and 296 K). Crystallographic data and experimental parameters are summarized in Table 1. The structures were determined by the direct method (SAPI 91 for **1**, SIR 92 for **2** and **3**),[13] and refined by full-matrix least-squares techniques. In **2**$Br_3\cdot H_2O$ two sets of atoms corresponding to a pair of enantiomers co-exist in the unit cell. Anisotropic thermal parameters were used for non-hydrogen atoms except N(1) and C(1–12) in **2**$Br_3\cdot H_2O$. The hydrogen atoms on the aet ligands were fixed by geometrical and thermal constraints (C–H = N–H 0.95 Å and $U = 1.3U$(C, N)). All the calculations were performed on an Indigo II computer using the TEXSAN crystallographic software package.[14]

CCDC reference number 186/1853.

See http://www.rsc.org/suppdata/dt/a9/a906665i/ for crystallographic files in .cif format.

Results and discussion

Syntheses

The reaction of *fac*(*S*)-[Ir(aet)$_3$] with a half equivalent of molybdenum(III) ion exposed to air in acid at room temperature gave the linear-type S-bridged trinuclear $Ir^{III}Mo^{IV}Ir^{III}$ complex, *meso*-$[Mo^{IV}\{Ir(aet)_3\}_2]^{4+}$ **1** (Scheme 1). Namely, the central molybdenum(IV) ion, which does not retain the oxidation state of the starting $[Mo^{III}Cl_5(H_2O)]^{2-}$, is incorporated into the polynuclear structure. Since a similar reaction under a nitrogen atmosphere also produced **1**, the oxidation of Mo^{III} in this reaction would be effected by acid as observed in the formation of $[Ir_2(aet)_4(cysta)]^{2+}$ (cysta = cysteamine).[15] On the other hand, the reaction of *fac*(*S*)-[Rh(aet)$_3$] with Mo^{III} in acid under both anaerobic and aerobic atmospheres gave the trinuclear Rh^{III}-$Mo^{III}Rh^{III}$ complex, *rac*-$[Mo^{III}\{Rh(aet)_3\}_2]^{3+}$ **2** (Scheme 1). In this reaction, the central Mo^{III} retains the oxidation state of the starting complex. Thus, the oxidation states for the central molybdenum ion in the trinuclear complexes are different, depending upon the metal ions in the terminal building blocks, *fac*(*S*)-[M(aet)$_3$]. In addition, only one of the *meso* or *rac* isomers was obtained in the present trinuclear complexes in each case. This is in contrast to the fact that both isomers of the corresponding trinuclear $MCr^{III}M$ complexes, *meso*- and *rac*-$[Cr^{III}\{M(aet)_3\}_2]^{3+}$ (M = Ir^{III} or Rh^{III}), were formed by the reaction of *fac*(*S*)-[M(aet)$_3$] with Cr^{III}.[7] The calculated structural energies (MM2 program) for linear-type S-bridged trinuclear complexes indicate little difference between these isomers. Accordingly, it is assumed that although both isomers exist in the reaction mixture, the less soluble isomer (*meso* for Ir and *rac* for Rh) is crystallized. It is also possible that the crystallization is accompanied by isomerization, as in the case of $[Ni^{II}\{M(aet)_3\}_2]^{2+}$ (M = Rh^{III}, Co^{III}, or Cr^{III}).[5,16]

In the reaction of *fac*(*S*)-[Rh(aet)$_3$] with Mo^{III} in acid in air at room temperature the mixture was changed from green-brown to wine-red gradually. From the wine-red suspension, an unprecedented S-bridged pentanuclear $Rh^{III}{}_3Mo^{V}{}_2$ complex, $[Mo^{V}{}_2O_2(\mu\text{-}O)\{Rh(aet)_3\}_3]^{4+}$ **3**, was obtained (Scheme 1). In a similar reaction under nitrogen, the mixture remained green-brown at least for 1 d. Namely, the molybdenum(III) complex **2**

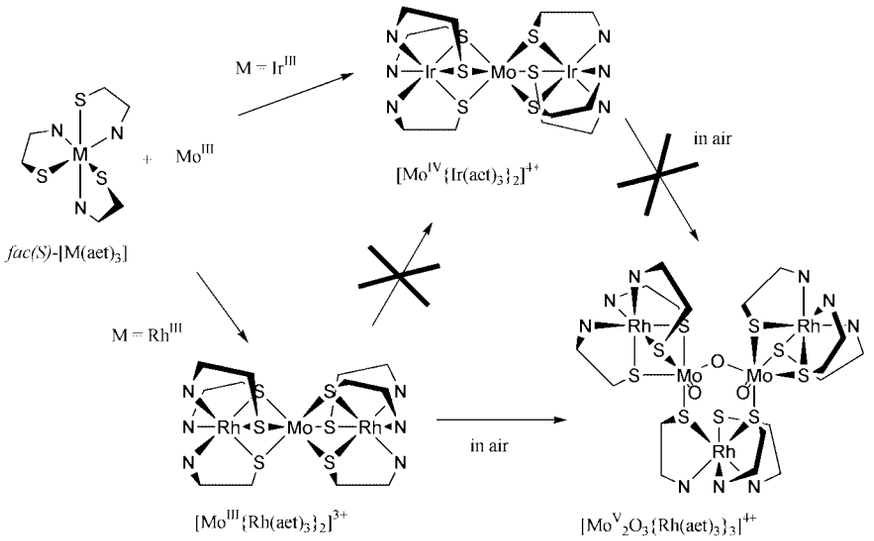

Scheme 1

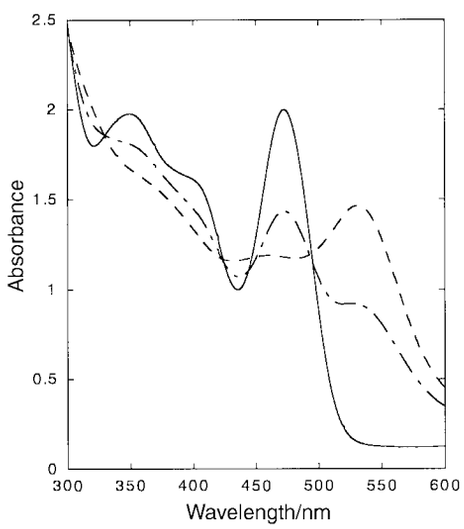

Fig. 1 Absorption spectral changes with times of $[Mo\{Rh(aet)_3\}_2]^{3+}$ **2**; 0 (———), 4 (—·—), and 16 h (– – – –).

is spontaneously oxidized by air and changed to the molybdenum(v) complex **3**. It has been reported that the doubly bridged $Mo_2O_2(\mu\text{-}O)_2^{2+}$ core is preponderant in dilute (*ca.* 1 mol dm^{-3}) acid conditions.[17] In this case, we might expect formation of a tetranuclear structure such as $[Mo^V_2O_2(\mu\text{-}O)_2\{Rh(aet)_3\}_2]^{2+}$.[18] However, **3** has the singly bridged $Mo_2O_2(\mu\text{-}O)^{4+}$ core, which predominates in 3–5 mol dm^{-3} acid solution, resulting in the more complicated pentanuclear structure, $[Mo^V_2O_2(\mu\text{-}O)\{Rh(aet)_3\}_3]^{4+}$. Accordingly, assembly of the present structure could be controlled by *fac*(*S*)-$[Rh(aet)_3]$ units as building blocks. Structural conversion from **2** into **3** in water was monitored by their UV-vis absorption spectra. As shown in Fig. 1, the absorbance of the characteristic intense band at 473 nm for **2** decreased and that at 529 nm for **3** increased. In this oxidation reaction, since the ratio of Rh and Mo atoms in the polynuclear structure changes from 2:1 to 3:2, the resulting excess of *fac*(*S*)-$[Rh(aet)_3]$ was deposited as a yellow powder. Although a similar experiment for the trinuclear $Ir^{III}Mo^{IV}Ir^{III}$ complex **1** was also attempted, the formation of the corresponding pentanuclear complex could not be observed (Scheme 1). This means that a further electrochemical difference depending upon the terminal building blocks was observed.

Structures

The perspective drawings of the entire complex cations **1** and **2**

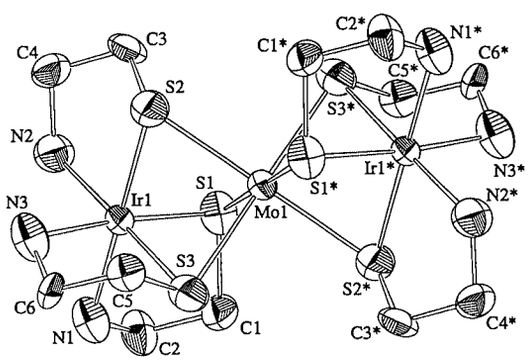

Fig. 2 Perspective view of ΔΛ-$[Mo\{Ir(aet)_3\}_2]^{4+}$ **1** with the atomic labeling scheme.

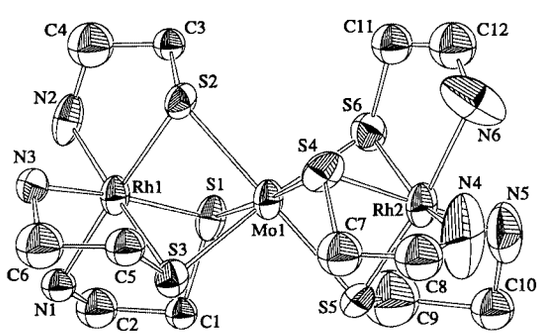

Fig. 3 Perspective view of ΔΔ-$[Mo\{Rh(aet)_3\}_2]^{3+}$ **2** with the atomic labeling scheme. The overlapped ΛΛ isomer is omitted for clarity.

are given in Figs. 2 and 3, respectively. Selected bond distances and angles are listed in Tables 2 and 3. Both **1** and **2** consist of two approximately octahedral *fac*(*S*)-$[M(aet)_3]$ ($M = Ir^{III}$ **1** or Rh^{III} **2**) units and one central molybdenum atom. These are consistent with plasma emission spectral analysis, which gave a value of M : Mo = 2 : 1. The overall structures of both **1** and **2**, in which the molybdenum atom is co-ordinated by the three thiolato sulfur atoms from each *fac*(*S*)-$[M(aet)_3]$ unit, are similar to those of the previously reported linear-type S-bridged trinuclear complexes, $[M'\{M(aet)_3\}_2]^{n+}$ ($M' = Cr^{III}$, Co^{III}, or Ni^{II}).[5–7] However, the total number of bromide anions implies that the entire complex cation **1** is tetravalent, while the cation **2** is trivalent. Namely, the oxidation states of the molybdenum ion in **1** and **2** are tetravalent and trivalent, respectively. These differences are supported by the results of the elemental analyses and molar conductivities. Observed molar conductivities

Table 1 Crystallographic data for $[Mo\{Ir(aet)_3\}_2]Br_4\cdot 4H_2O$ ($\mathbf{1}Br_4\cdot 4H_2O$), $[Mo\{Rh(aet)_3\}_2]Br_3\cdot H_2O$ ($\mathbf{2}Br_3\cdot H_2O$) and $[Mo_2O_2(\mu\text{-}O)\{Rh(aet)_3\}_3]Br_4\cdot 6H_2O$ ($\mathbf{3}Br_4\cdot 6H_2O$)

	$\mathbf{1}Br_4\cdot 4H_2O$	$\mathbf{2}Br_3\cdot H_2O$	$\mathbf{3}Br_4\cdot 6H_2O$
Formula	$C_{12}H_{44}Br_4Ir_2MoN_6O_4S_6$	$C_{12}H_{38}Br_3MoN_6ORh_2S_6$	$C_{18}H_{66}Br_4Mo_2N_9O_9Rh_3S_9$
Formula weight	1328.87	1016.29	1661.53
Crystal system	Monoclinic	Orthorhombic	Triclinic
Space group	$P2_1/n$ (no. 14)	$Pnma$ (no. 62)	$P\bar{1}$ (no. 2)
a/Å	11.530(3)	17.125(7)	14.236(5)
b/Å	12.026(2)	12.450(5)	14.917(3)
c/Å	12.577(2)	14.184(4)	13.622(2)
α/°			114.81(1)
β/°	90.45(2)		95.57(2)
γ/°			82.46(3)
V/Å^3	1743.9(6)	3024(1)	2600(1)
Z	2	4	2
D_{calc}/g cm^{-3}	2.530	2.232	2.122
μ(Mo-Kα)/cm^{-1}	129.71	58.92	48.89
Measured reflections	4204	3900	12433
Independent reflections	4204	3899	11954
Observed reflections ($>3\sigma I_o$)	2597	1209	5987
Parameters	160	184	466
Final R, R_w	0.072, 0.095	0.056, 0.070	0.043, 0.055

Table 2 Selected bond distances (Å) and angles (°) for $[Mo\{Ir(aet)_3\}_2]^{4+}$ **1**

Ir(1)···Mo(1)	2.7469(7)	Ir(1)–N(2)	2.08(2)
Ir(1)–S(1)	2.340(7)	Ir(1)–N(3)	2.11(2)
Ir(1)–S(2)	2.332(6)	Mo(1)–S(1)	2.455(7)
Ir(1)–S(3)	2.352(7)	Mo(1)–S(2)	2.456(6)
Ir(1)–N(1)	2.11(2)	Mo(1)–S(3)	2.463(6)
S(1)–Ir(1)–S(2)	94.5(2)	S(1)–Mo(1)–S(2)	88.6(2)
S(1)–Ir(1)–S(3)	92.4(2)	S(1)–Mo(1)–S(3)	87.0(2)
S(2)–Ir(1)–S(3)	93.0(2)	S(2)–Mo(1)–S(3)	87.4(2)
N(1)–Ir(1)–N(2)	93.9(8)	Ir(1)–S(1)–Mo(1)	69.9(2)
N(1)–Ir(1)–N(3)	89.8(8)	Ir(1)–S(2)–Mo(1)	70.0(2)
N(2)–Ir(1)–N(3)	92.5(9)	Ir(1)–S(3)–Mo(1)	69.5(2)

Table 3 Selected bond distances (Å) and angles (°) for $[Mo\{Rh(aet)_3\}_2]^{3+}$ **2**

Rh(1)···Mo(1)	2.852(3)	Rh(2)···Mo(1)	2.867(3)
Rh(1)–S(1)	2.366(9)	Rh(2)–S(4)	2.41(1)
Rh(1)–S(2)	2.282(9)	Rh(2)–S(5)	2.228(10)
Rh(1)–S(3)	2.347(8)	Rh(2)–S(6)	2.353(9)
Rh(1)–N(1)	2.17(3)	Rh(2)–N(4)	2.04(3)
Rh(1)–N(2)	2.07(3)	Rh(2)–N(5)	2.03(4)
Rh(1)–N(3)	2.02(3)	Rh(2)–N(6)	2.21(4)
Mo(1)–S(1)	2.445(9)	Mo(1)–S(4)	2.432(10)
Mo(1)–S(2)	2.437(8)	Mo(1)–S(5)	2.477(9)
Mo(1)–S(3)	2.433(9)	Mo(1)–S(6)	2.43(1)
S(1)–Rh(1)–S(2)	91.2(3)	S(1)–Mo(1)–S(2)	85.7(3)
S(1)–Rh(1)–S(3)	88.2(3)	S(1)–Mo(1)–S(3)	84.5(3)
S(2)–Rh(1)–S(3)	91.7(3)	S(2)–Mo(1)–S(3)	86.0(3)
N(1)–Rh(1)–N(2)	93(1)	S(4)–Mo(1)–S(5)	84.0(3)
N(1)–Rh(1)–N(3)	91.7(10)	S(4)–Mo(1)–S(6)	87.3(4)
N(2)–Rh(1)–N(3)	93(1)	S(5)–Mo(1)–S(6)	83.8(3)
S(4)–Rh(2)–S(5)	90.2(4)	Rh(1)–S(1)–Mo(1)	72.7(3)
S(4)–Rh(2)–S(6)	89.5(3)	Rh(1)–S(2)–Mo(1)	74.3(3)
S(5)–Rh(2)–S(6)	91.2(3)	Rh(1)–S(3)–Mo(1)	73.2(3)
N(4)–Rh(2)–N(5)	102(1)	Rh(2)–S(4)–Mo(1)	72.7(3)
N(4)–Rh(2)–N(6)	81.6(9)	Rh(2)–S(5)–Mo(1)	74.9(3)
N(5)–Rh(2)–N(6)	95(1)	Rh(2)–S(6)–Mo(1)	73.7(3)

of **1** and **2** were *ca.* 400 and 600 S cm^2 mol^{-1}, respectively. Accurate values could not be obtained because of instability in dilute solution. The Ir···Mo^{IV} distances in **1** (2.7469(7) Å) are significantly shorter than the Rh···Mo^{III} distances in **2** (average 2.860(3) Å). The corresponding M···Cr^{III} distances in ΔΛ-$[Cr\{M(aet)_3\}_2]^{3+}$ (M = Ir^{III}, 2.9096(3) Å and Rh^{III}, 2.9328(2) Å)[7] show no significant structural differences depending upon the terminal *fac*(*S*)-[M(aet)$_3$] units. Therefore, the difference of M···Mo distances in **1** and **2** reflects the oxidation state of the central molybdenum ion. On the other hand, the M···Mo distances in **1** and **2** are significantly shorter than the M···Cr distances in the chromium(III) complexes. In particular, the Ir···Mo^{IV} distances in **1** are the shortest M···M′ separations of any reported $[M'\{M(aet)_3\}_2]^{n+}$.[5–7] The S–M–S bite angles in the terminal *fac*(*S*)-[M(aet)$_3$] units (average 93.3(2)° in **1** and 90.3(4)° in **2**) are obtuse, compared with those in other $[M'\{M(aet)_3\}_2]^{n+}$ (<90°).[5–7] Further, the bridging M–S–Mo bite angles (average 69.8(2)° in **1** and 73.6(3)° in **2**) are acute, compared with those in other $[M'\{M(aet)_3\}_2]^{n+}$ (>75°).[5–7] These facts indicate that the terminal *fac*(*S*)-[M(aet)$_3$] units are strongly attracted by the central molybdenum ion.

Considering the absolute configurations (Δ and Λ) of the two terminal *fac*(*S*)-[M(aet)$_3$] units, three isomers (ΔΔ, ΛΛ, and ΔΛ) are possible for $[Mo\{M(aet)_3\}_2]^{n+}$. The cation **1** consists of the ΔΛ (*meso*) isomer, with the crystallographic inversion center located on the central molybdenum atom. On the other hand, the cation **2** consists of the ΔΔ and ΛΛ (*rac*) isomers, although only the ΔΔ isomer is illustrated in Fig. 3. In the unit cell the ΔΔ and ΛΛ isomers of **2** co-exist in each of four sites with a site occupancy of 0.5 and some distortion of structure was observed, which was similar to that observed in ΔΔ/ΛΛ-$[Ag_3\{M(aet)_3\}_2]^{3+}$ (M = Rh^{III} or Co^{III}).[2] This indicates that **2** is not a racemic compound but a rare example of a racemic solid solution.[19] All the bridging sulfur atoms in **1** and **2** are fixed to the *R* configuration for the Δ unit and the *S* configuration for the Λ unit, as observed in ΔΛ-$[Cr\{M(aet)_3\}_2]^{3+}$[7] or ΔΔ/ΛΛ-$[Ni\{Rh(aet)_3\}_2]^{2+}$.[5]

A perspective drawing of the cation **3** is given in Fig. 4, and selected bond distances and angles are listed in Table 4. The presence of four bromide anions and the result of the elemental analysis indicate that **3** is tetravalent, which means that each molybdenum ion is pentavalent. The cation **3** consists of three approximately octahedral *fac*(*S*)-[Rh(aet)$_3$] units, retaining the structure of the starting mononuclear complex, and a $Mo_2O_2(\mu\text{-}O)^{4+}$ core, bridged by one oxygen atom. This is consistent with the plasma emission spectral analysis which gave a value of Rh : Mo = 3 : 2. In the central $Mo_2O_2(\mu\text{-}O)^{4+}$ core the Mo(1)–O(1) and Mo(2)–O(2) distances (average 1.676(7) Å) imply double bonds and the O(1) and O(2) atoms are *anti* to one another. The Mo(1)–O(3) and Mo(2)–O(3) distances average 1.870(6) Å, suggesting single bonds. The Mo···Mo distance (3.664(1) Å) in **3** is longer than those in complexes containing a $Mo_2O_2(\mu\text{-}O)_2^{2+}$ core bridged by two oxygen atoms.[20] Although the Mo–O–Mo angles in most complexes containing a

Table 4 Selected bond distances (Å) and angles (°) for $[Mo_2O_2(\mu\text{-}O)\{Rh(aet)_3\}_3]^{4+}$ **3**

Rh(1)···Mo(1)	3.165(1)	Rh(2)···Mo(2)	3.229(1)
Rh(3)···Mo(1)	4.127(1)	Rh(3)···Mo(2)	4.121(1)
Rh(1)–S(1)	2.310(3)	Rh(2)–S(4)	2.302(2)
Rh(1)–S(2)	2.324(3)	Rh(2)–S(5)	2.306(3)
Rh(1)–S(3)	2.315(2)	Rh(2)–S(6)	2.313(3)
Rh(1)–N(1)	2.083(8)	Rh(2)–N(4)	2.078(8)
Rh(1)–N(2)	2.107(8)	Rh(2)–N(5)	2.107(8)
Rh(1)–N(3)	2.100(9)	Rh(2)–N(6)	2.101(8)
Mo(1)–S(1)	2.738(3)	Mo(2)–S(4)	2.778(3)
Mo(1)–S(2)	2.565(2)	Mo(2)–S(5)	2.518(2)
Mo(1)–S(3)	2.459(3)	Mo(2)–S(6)	2.541(3)
Mo(1)–S(7)	2.458(2)	Mo(2)–S(8)	2.439(3)
Rh(3)–S(7)	2.315(2)	Mo(1)–O(1)	1.671(7)
Rh(3)–S(8)	2.334(3)	Mo(1)–O(3)	1.875(6)
Rh(3)–S(9)	2.318(3)	Mo(2)–O(2)	1.681(7)
Rh(3)–N(7)	2.102(9)	Mo(2)–O(3)	1.864(6)
Rh(3)–N(8)	2.112(8)	Rh(3)–N(9)	2.107(8)
Mo(1)···Mo(2)	3.664(1)		
S(1)–Rh(1)–S(2)	88.34(9)	S(1)–Mo(1)–S(2)	74.93(8)
S(1)–Rh(1)–S(3)	89.47(9)	S(1)–Mo(1)–S(3)	77.34(8)
S(2)–Rh(1)–S(3)	87.50(9)	S(2)–Mo(1)–S(3)	79.35(8)
N(1)–Rh(1)–N(2)	92.2(3)	S(7)–Mo(1)–O(1)	100.1(2)
N(1)–Rh(1)–N(3)	94.4(3)	S(7)–Mo(1)–O(3)	94.6(2)
N(2)–Rh(1)–N(3)	94.8(3)	O(1)–Mo(1)–O(3)	104.5(3)
S(4)–Rh(2)–S(5)	87.81(9)	O(1)–Mo(1)–S(1)	172.1(2)
S(4)–Rh(2)–S(6)	87.29(9)	O(1)–Mo(1)–S(2)	97.3(2)
S(5)–Rh(2)–S(6)	88.06(9)	O(1)–Mo(1)–S(3)	100.2(2)
N(4)–Rh(2)–N(5)	93.8(3)	S(4)–Mo(2)–S(5)	74.02(8)
N(4)–Rh(2)–N(6)	93.5(3)	S(4)–Mo(2)–S(6)	73.42(8)
N(5)–Rh(2)–N(6)	95.8(3)	S(5)–Mo(2)–S(6)	78.77(8)
S(7)–Rh(3)–S(8)	100.24(9)	S(8)–Mo(2)–O(2)	103.5(3)
S(7)–Rh(3)–S(9)	91.73(9)	S(8)–Mo(2)–O(3)	87.4(2)
S(8)–Rh(3)–S(9)	95.04(10)	O(2)–Mo(2)–O(3)	108.1(3)
N(7)–Rh(3)–N(8)	92.9(3)	O(2)–Mo(2)–S(4)	164.6(2)
N(7)–Rh(3)–N(9)	92.0(3)	O(2)–Mo(2)–S(5)	96.0(2)
N(8)–Rh(3)–N(9)	88.6(3)	O(2)–Mo(2)–S(6)	93.3(3)
Rh(1)–S(1)–Mo(1)	77.14(7)	Rh(2)–S(4)–Mo(2)	78.32(8)
Rh(1)–S(2)–Mo(1)	80.52(8)	Rh(2)–S(5)–Mo(2)	83.92(8)
Rh(1)–S(3)–Mo(1)	83.01(8)	Rh(2)–S(6)–Mo(2)	83.26(8)
Rh(3)–S(7)–Mo(1)	119.68(10)	Rh(3)–S(8)–Mo(2)	119.4(1)
Mo(1)–O(3)–Mo(2)	157.0(4)		

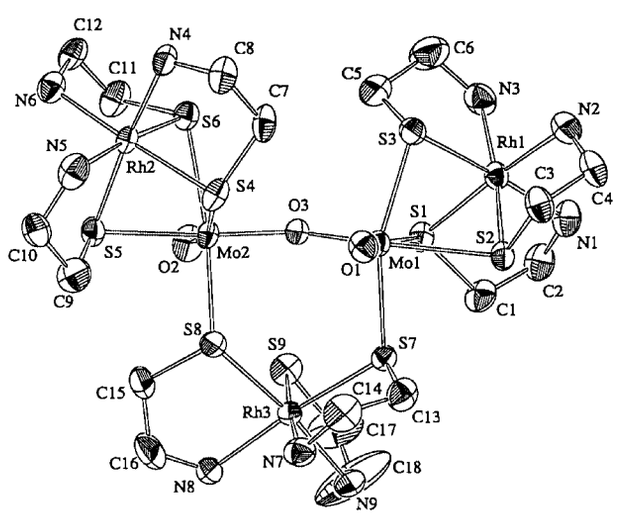

Fig. 4 Perspective view of ΛΔΔ-$[Mo_2O_2(\mu\text{-}O)\{Rh(aet)_3\}_3]^{4+}$ **3** with the atomic labeling scheme.

$Mo_2O_2(\mu\text{-}O)^{4+}$ core are close to 180°,[21] the Mo–O–Mo angle (157.0(4)°) in **3** is unique.

Each Rh(1) and Rh(2) unit in complex **3** is bound to one molybdenum atom, while the Rh(3) unit bridges two molybdenum atoms. The bond distances and angles in the Rh(1) and Rh(2) units are within the approximate ranges observed previously for the *fac*(*S*)-[Rh(aet)$_3$] unit, whose three thiolato sulfur atoms co-ordinate to the same metal.[3,5,7] However, the Rh(3) unit is distorted from regular geometry. In particular, the S(7)–Rh(3)–S(8) angle (100.24(9)°) is significantly deviated from 90°, and much larger than that in *fac*(*S*)-[Rh(aet)$_3$] units whose three thiolato sulfur atoms co-ordinate to different metals.[1–3] The corresponding N(8)–Rh(3)–N(9) angle (88.6(3)°) is acuter than other N–Rh–N ones. This seems to reflect that two sulfur atoms in the Rh(3) unit are bound to two molybdenum atoms, and S(9) remains as a non-bridging thiolato sulfur atom. The Mo(1)–S(1) and Mo(2)–S(4) distances *trans* to the Mo–O double bonds (average 2.758(3) Å) are much longer than the other Mo–S (average 2.497(3) Å). This can be considered due to a *trans* influence, and similar lengthening was observed in some dinuclear molybdenum complexes.[21] Owing to the lengthening of the Mo–S bonds, the Rh(1)–Mo(1) and Rh(2)–Mo(2) distances (3.165(1) and 3.229(1) Å, respectively) are longer than the Rh–M′ distances in the trinuclear complexes $[M'\{M(aet)_3\}_2]^{n+}$ (2.9328(2)–2.9451(5) Å).[5,7]

Considering the absolute configurations of the three terminal *fac*(*S*)-[M(aet)$_3$] units, the cation **3** consists of a pair of enantiomers, Δ(Rh1)Λ(Rh2)Λ(Rh3) and Λ(Rh1)Δ(Rh2)Δ(Rh3), which combine to form the racemic compound, although the ΛΔΔ isomer is illustrated in Fig. 4. All the bridging sulfur atoms in **3** are also fixed to the *R* configuration for the Δ unit and the *S* configuration for the Λ unit, similar to those in **1** and **2**.

Table 5 Electronic absorption spectral data of the complexes

Complex	Absorption maxima $\sigma/10^3$ cm^{-1} (log ε/dm^3 mol^{-1} cm^{-1})
1 $[Mo\{Ir(aet)_3\}_2]^{4+}$	13.91 (2.88), 18.03 (3.29), 22.22 (3.66), 24.27 (3.58), 34.5 (3.9sh[a]), 41.0 (4.2sh), 50.63 (4.90)
2 $[Mo\{Rh(aet)_3\}_2]^{3+}$	15.04 (2.60), 21.16 (3.74), 24.97 (3.64), 28.57 (3.73), 37.2 (4.1sh), 45.9 (4.8sh)
3 $[Mo_2O_2(\mu\text{-}O)\{Rh(aet)_3\}_3]^{4+}$	15.1 (3.2sh), 18.90 (3.77), 28.3 (3.9sh), 44.25 (5.13)

[a] sh denotes a shoulder.

Properties

The electronic absorption spectral data of complexes **1**–**3** are summarized in Table 5. In the UV region the most intense band at *ca.* 50×10^3 cm^{-1} for **1** corresponds well to sulfur-to-iridium charge transfer bands as observed for complexes involving *fac*(*S*)-[Ir(aet)$_3$] units.[6] Similarly, the most intense bands at *ca.* 45×10^3 cm^{-1} for **2** and **3** correspond well to sulfur-to-rhodium charge transfer bands.[4] In the visible region, the characteristic intense bands at (20–25) $\times 10^3$ cm^{-1} for **1**–**3** can be assigned as arising from the central $Mo^{IV}S_6$, $Mo^{III}S_6$, or $Mo^{V}{}_2O_3S_8$ chromophore, because the terminal $Ir^{III}N_3S_3$ or $Rh^{III}N_3S_3$ chromophores show less absorption bands in this visible region.[4]

The infrared spectrum of complex **1** coincides well with that of **2** (Table 6). This clearly reflects the similarity of their overall structures. On the other hand, **3** exhibits a characteristic strong band at 949 cm^{-1}, due to the symmetric stretching vibration mode of the Mo–O double bonds,[22] and a similar band was not observed in the spectra of **1** and **2**. The Raman spectrum of **3** exhibits also a corresponding band at 943 cm^{-1}. Moreover, its spectrum indicates some shifts of those bands which are assigned as the *fac*(*S*)-[Rh(aet)$_3$] units, as well as new bands which depend upon the $Mo_2O_2(\mu\text{-}O)^{4+}$ core. Thus, these results support our observation that the $Mo_2O_2(\mu\text{-}O)^{4+}$ core was incorporated into the S-bridged polynuclear structure.

The magnetic moment of complex **1** (2.71 μ_B) at room temperature is in agreement with that expected from the central molybdenum(IV) ion, which has d^2 electronic structure. However, **2** has a lower magnetic moment (2.04 μ_B) than that expected from the central Mo^{III}, which has d^3 electronic

Table 6 Infrared and Raman spectral data of the complexes

Complex	$\tilde{\nu}$/cm^{-1}
1 $[Mo\{Ir(aet)_3\}_2]^{4+}$	
Infrared	3436s, 3142vs, 3019vs, 1615w, 1587s, 1450w, 1419m, 1387w, 1318m, 1268m, 1233w, 1167m, 1115w, 1032w, 983m, 918w, 843w, 759w, 652w, 524w
2 $[Mo\{Rh(aet)_3\}_2]^{3+}$	
Infrared	3391s, 3172vs, 3083vs, 2945w, 2910w, 1646w, 1579s, 1448m, 1418m, 1377w, 1307w, 1265m, 1227w, 1142m, 1098w, 1034w, 977m, 916w, 840w, 740w, 644w, 525w, 419w
3 $[Mo_2O_2(\mu\text{-}O)\{Rh(aet)_3\}_3]^{4+}$	
Infrared	3428 (br), 3206vs, 3116vs, 2923w, 1582s, 1453w, 1419m, 1302w, 1270m, 1234w, 1133m, 1102w, 1035w, 977m, 949s, 918w, 847w, 731w, 657w, 519w, 423w, 404w
Raman	1826 (br), 1692w, 1598w, 1459m, 1378w, 1307w, 1274w, 1243w, 1163w, 1137w, 1105w, 1046w, 978w, 956m, 943vs, 925w, 902w, 851w, 789w, 734m, 662m, 541w, 530w, 482w, 449s, 425m, 391s, 363w, 330w, 278w, 270w, 248s, 207vs

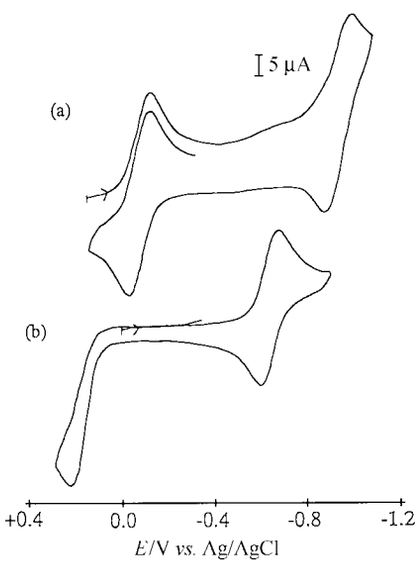

Fig. 5 Cyclic voltammograms of (a) $[Mo\{Ir(aet)_3\}_2]^{4+}$ **1** and (b) $[Mo\{Rh(aet)_3\}_2]^{3+}$ **2**; scan rate 200 mV s^{-1}.

structure. It was reported that mononuclear molybdenum(III) complexes ligated by some nitrogen donors exhibit magnetic moments of 3.64–3.74 μ_B.[23] The low magnetic moment of **2** might be related to a considerably distorted trinuclear structure resulting in a low-spin arrangement with one unpaired electron, although details are not at all clear. The pentanuclear complex **3** is diamagnetic although it contains molybdenum(V) ions, which have d^1 electronic structure. Molybdenum polynuclear complexes containing $Mo_2O_2(\mu\text{-}O)^{4+}$ or $Mo_2O_2(\mu\text{-}O)_2^{2+}$ cores commonly show low or no magnetic moment.[22] The long Mo···Mo distance (3.664(1) Å) implies the absence of direct metal–metal interaction, that is antiferromagnetic superexchange coupling through the bridging oxo oxygen atom is expected.

The cyclic voltammograms of $[Mo^{IV}\{Ir^{III}(aet)_3\}_2]^{4+}$ **1** and $[Mo^{III}\{Rh^{III}(aet)_3\}_2]^{3+}$ **2** are shown in Fig. 5. Since it is known that the redox process concerned with the terminal *fac*(*S*)-$[M(aet)_3]$ (M = Ir^{III} or Rh^{III}) units does not occur in the potential region +0.3 to −1.1 V (*vs.* Ag–AgCl) for their corresponding trinuclear complexes, $[M'\{M(aet)_3\}_2]^{3+}$ (M′ = Co^{III} or Cr^{III}),[6,7] all displayed waves in Fig. 5 can be regarded as redox processes of the central molybdenum ion. The reversible redox processes with 0.10 V peak–peak separations at a negative potential region ($E^{\circ\prime}$ = −0.96 V for **1** and −0.65 V for **2**) probably involve the central Mo^{III}–Mo^{II} couple. This is in contrast to the fact that Cr^{III}–Cr^{II} processes of the corresponding $[Cr^{III}\{M(aet)_3\}_2]^{3+}$ are irreversible.[7] The reversible redox process with a 0.10 V peak–peak separation for **1**, involving Mo^{IV}–Mo^{III} appears at $E^{\circ\prime}$ = −0.08 V. On the contrary, **2** exhibits an irreversible oxidation wave at the positive region (E_{pa} = +0.23 V). These facts suggest that **1** can exist as a trinuclear complex involving the molybdenum(IV) ion, whereas **2** exists as a trinuclear complex involving molybdenum(III) ion and cannot retain this structure upon oxidation. Moreover, from the potential differences of the oxidation waves, it is reasonable to assume that the lower oxidation state of the central molybdenum ion is relatively stabilized in the rhodium complex **2**. Thus, the cyclic voltammetry experiments obviously showed the electrochemical difference of the molybdenum ions, which are incorporated into the S-bridged polynuclear structures, depending upon the kind of building block, *fac*(*S*)-$[M(aet)_3]$.

References

1 (*a*) T. Konno, K. Okamoto and J. Hidaka, *Inorg. Chem.*, 1991, **30**, 2253; (*b*) T. Konno, K. Okamoto and J. Hidaka, *Inorg. Chem.*, 1994, **33**, 538; (*c*) T. Konno, Y. Kageyama and K. Okamoto, *Bull. Chem. Soc. Jpn.*, 1994, **67**, 1957; (*d*) K. Okamoto, T. Konno, Y. Kageyama and J. Hidaka, *Chem. Lett.*, 1992, 1105; (*e*) K. Okamoto, Y. Kageyama and T. Konno, *Bull. Chem. Soc. Jpn.*, 1995, **68**, 2573; (*f*) K. Okamoto, T. Konno and J. Hidaka, *J. Chem. Soc.*, *Dalton Trans.*, 1994, 533.

2 T. Konno and K. Okamoto, *Inorg. Chem.*, 1997, **36**, 1403; T. Konno, K. Tokuda, T. Suzuki and K. Okamoto, *Bull. Chem. Soc. Jpn.*, 1998, **71**, 1049.

3 T. Konno, C. Sasaki and K. Okamoto, *Chem. Lett.*, 1996, 977; K. Okamoto, C. Sasaki, Y. Yamada and T. Konno, *Bull. Chem. Soc. Jpn.*, 1999, **72**, 1685.

4 T. Konno, S. Aizawa, K. Okamoto and J. Hidaka, *Bull. Chem. Soc. Jpn.*, 1990, **63**, 792.

5 T. Konno and K. Okamoto, *Bull. Chem. Soc. Jpn.*, 1995, **68**, 610.

6 T. Konno, K. Nakamura, K. Okamoto and J. Hidaka, *Bull. Chem. Soc. Jpn.*, 1993, **66**, 2582.

7 Y. Miyashita, N. Sakagami, Y. Yamada, T. Konno, J. Hidaka and K. Okamoto, *Bull. Chem. Soc. Jpn.*, 1998, **71**, 661.

8 T. Shibahara, *Coord. Chem. Rev.*, 1993, **123**, 73; M. J. Morris, *Coord. Chem. Rev.*, 1998, **172**, 181.

9 T. Shibahara and M. Yamazaki, *Bull. Chem. Soc. Jpn.*, 1990, **63**, 3022.

10 M. Kita, K. Yamanari and Y. Shimura, *Bull. Chem. Soc. Jpn.*, 1983, **56**, 3272.

11 *Landolt-Börnstein Tabellen*, Neue Serie, II Band, 2 Teil, Springer, Berlin, 1966.

12 CAChe, Version 3.7, CAChe Scientific, Inc, Tokyo, Japan, 1994.

13 SAPI91, Fan Hai-Fu, Structure Analysis Programs with Intelligent Control, Rigaku Corporation, Tokyo, Japan, 1991; SIR 92, A. Altomare, M. C. Burla, M. Camalli, M. Cascarano, C. Giacovazzo, A. Guagliardi and G. Polidori, *J. Appl. Crystallogr.*, 1994, **27**, 435.

14 TEXSAN, Single Crystal Structure Analysis Software, Version 1.8, Molecular Structure Corporation, The Woodlands, TX, 1997.

15 T. Konno, Y. Miyashita and K. Okamoto, *Chem. Lett.*, 1997, 85; Y. Miyashita, N. Sakagami, Y. Yamada, T. Konno and K. Okamoto, *Bull. Chem. Soc. Jpn.*, 1998, **71**, 2153.

16 T. Konno, K. Okamoto and J. Hidaka, *Acta Crystallogr.*, *Sect. C*, 1993, **49**, 222; K. Okamoto, M. Matsumoto, Y. Miyashita, N. Sakagami, J. Hidaka and T. Konno, *Inorg. Chim. Acta*, 1997, **260**, 17.

17 S. Himeno and M. Hasegawa, *Inorg. Chim. Acta*, 1984, **83**, L17.
18 R. Xi, B. Wang, M. Abe, Y. Ozawa, I. Kinoshita and K. Isobe, *Bull. Chem. Soc. Jpn.*, 1999, **72**, 1985.
19 J. Jacques, A. Collet and S. H. Wilen, *Enantiomers, Racemates and Resolutions*, John Wiley & Sons, New York, 1981.
20 R. H. Holm, *Chem. Rev.*, 1987, **87**, 1401.
21 J. R. Knox and C. K. Prout, *Acta Crystallogr.*, *Sect. B*, 1969, **25**, 2281; J. A. Zubieta and G. B. Maniloff, *Inorg. Nucl. Chem. Lett.*, 1976, **12**, 121.
22 R. Lozano, J. Román, F. de Jesús and E. Alarcón, *Transition Met. Chem.*, 1990, **15**, 141; J. F. Johnson and W. R. Scheidt, *Inorg. Chem.*, 1978, **17**, 1280.
23 S. P. Ghosh and K. M. Prasad, *J. Less-Common Met.*, 1974, **36**, 223.

Paper a906665i